Available online at www.sciencedirect.com
SCIENCE DIRECT®
Journal of Molecular Spectroscopy 228 (2004) 143–151
Journal of MOLECULAR SPECTROSCOPY
www.elsevier.com/locate/jms

Three- and two-photon absorption in HCl and DCl: identification of Ω = 3 states and state interaction analysis

Ágúst Kvaran*, Huasheng Wang

Science Institute, University of Iceland, Dunhaga 3, 107 Reykjavík, Iceland

Received 25 May 2004; in revised form 14 July 2004
Available online 23 August 2004

Abstract

High resolution (3 + 1) and (2 + 1)REMPI spectra of HCl and DCl for total current detection at room temperature or TOF mass detection after jet cooling were recorded for the spectral region 89 000–89 600 cm^{-1}. Analysis of the (3 + 1)REMPI spectra by use of three-photon absorption modeling allowed, for the first time, identification and characterization of the $l(^3\Phi_3)$ states. Consistent anomalies in spectral structures due to transitions to the $j(^3\Sigma^-)(0^+)$ state are interpreted as being due to interactions with the $V(^1\Sigma^+)$ ion-pair states. Interaction strengths are evaluated. Simulation analyses and determination of isotope shifts allowed evaluation of vibrational and rotational spectroscopic parameters for the $l(^3\Phi_3)$ and the $j(^3\Sigma^-)(0^+)$ states for both molecules.

1. Introduction

(3 + 1) and (2 + 1)REMPI (resonance-enhanced multiphoton ionization) involves three- and two-photon resonance absorption, respectively, followed by one-photon ionization. (n + 1)REMPI spectra of rotational structure in electronic transitions of diatomic molecules have been simulated successfully by taking account of the three-(n = 3) [1–5] and two-(n = 2) [6–11] photon transition probabilities only. This suggests that the final ionization step is largely wavelength independent and that the (n + 1)REMPI spectra (n = 2, 3) can be treated as n-photon absorption spectra to a first approximation. Furthermore, three-photon absorption spectroscopy analysis of (3 + 1)REMPI spectra has recently proven successful at detecting states "hidden" in the more commonly used single-, and two- photon absorption techniques [1,2,4,5]. Thus the lowest energy Ω = 3, Φ states of HBr ($l(^3\Phi_3)$; $\tilde{\nu}^0 = 80\,167\,cm^{-1}$ for $v' = 0$ and $L(^1\Phi_3)$; $\tilde{\nu}^0 = 82\,837\,cm^{-1}$ for $v' = 0$) [1,2] and the $L(^1\Phi_3)$ states of HCl and DCl $\tilde{\nu}^0 = 89981.6\,cm^{-1}$ for $v' = 0$ and $\tilde{\nu}^0 = 90\,055\,cm^{-1}$ for $v' = 0$, respectively) [4] were detected and analyzed in (3 + 1)REMPI spectra recorded at room temperature. A number of higher energy Ω = 3 (Φ) states for HBr were observed in cold supersonic expansions [5]. Three- and two-photon absorption spectroscopy has added to the rich spectroscopy of the hydrogen halides which is characterized by a wide variation in the strengths of Rydberg to ion-pair interactions as well as spin–orbit couplings arising from the halogen atoms [6,7,12–19]. Furthermore, use of expressions for rovibrational line strengths in three-photon absorption [1,2] has been found to be useful to derive rotational population distributions in the ground states of HBr [2] and HCl [3] from (3 + 1)REMPI spectra. The relative intensities of rotational line series have been used as evidence in debates about the effect of intermediate states on the mechanism of multiphoton processes in two- [6,7,20] and three-photon [2,4] absorptions to $\Omega' = 0 \leftarrow \Omega'' = 0$ transitions in Br_2 [20], HBr [7], and HCl [2,4,6,7].

In this paper, we present for the first time observation and analyses of electronic states in HCl and DCl which are not accessible in one- and two-photon spectra. Hönl-London expressions are used to identify and analyze

* Corresponding author. Fax: +354 552 8911.
E-mail address: agust@hi.is (Á. Kvaran).
URL: http://www.raunvis.hi.is/~agust/.

0022-2852/$ - see front matter © 2004 Elsevier Inc. All rights reserved.
doi:10.1016/j.jms.2004.07.014

$\Omega = 3$, Φ states of HCl from (3 + 1)REMPI room temperature spectra and of DCl from (3 + 1)REMPI spectra obtained after jet cooling. The states are assigned as the $l(^3\Phi_3)$ Rydberg states corresponding to the principal quantum number 3, belonging to the dδ manifold and state series converging to the $^2\Pi_{3/2}$ spin–orbit components of the ground state molecular ions. The analyses allowed determination of rotational and vibrational spectroscopic parameters for the excited electronic states.

Furthermore (3 + 1)REMPI spectra of HCl and DCl, involving three-photon transitions to the $j(^3\Sigma^-(0^+))$ states, are also recorded and analyzed for the first time. Clear evidence for near resonance interactions between the j and the $V(^1\Sigma^+)$ ion-pair states is seen both in the (3 + 1) and (2 + 1)REMPI spectra of HCl and DCl. The interaction strength is evaluated by model calculations [6], based on perturbation theory [21] and deperturbed energy levels [19].

2. Experimental

REMPI spectra of HCl were recorded at room temperature for samples in a static cell (REMPI-Current spectra) as described before [8,22,23]. REMPI spectra of DCl were recorded by detecting D $^{37}Cl^+$ ions in a time of flight mass spectrometer attached to an ionization chamber (REMPI-TOF spectra). Tunable radiation was generated by an excimer laser-pumped dye laser systems. REMPI-Current spectra were recorded by use of a Lumonics 510 excimer laser while REMPI-TOF spectra were recorded by use of a Lambda Physik COMPex 205 excimer laser. In both cases, a Lumonics Hyperdye 300 laser was used. The bandwidth of the dye laser beam was about 0.05 cm^{-1}. (2 + 1)REMPI spectra, for the wavelength range 223–225 nm, were obtained by using the dye C-440 and frequency doubling with a BBO-B crystal, but (3 + 1)REMPI spectra, over 334.5–337 nm, were obtained by using the dye LD-690 and a KDP-D crystal. The frequency-doubled beam was separated from the fundamental by a Pellin Broca prism.

The radiation was focused into an ionization cell between two stainless steel electrodes for recording HCl REMPI-Current spectra. The cell contained HCl gas samples (Merck, HCl: 99.5%) at low pressure, typically 1–5 Torr and room temperature after degassing by a series of freeze, pump, and thaw cycles. Current pulses in the gas due to laser pulse photoionization caused voltage drops across the electrodes. After amplification and integration the voltage pulses were fed into a LeCroy 9310A, 400 MHz storage oscilloscope. Finally, average voltage values for a fixed sampling time were recorded as a function of absorbed photon energy to get the spectrum. Typically spectral points were obtained by averaging over 100 pulses.

To avoid overlap signals due to HCl impurities, REMPI spectra of DCl were recorded after mass selection in a TOF mass spectrometer. The radiation was focused into an ionization chamber between a repeller and an extractor separated by 19 mm for recording DCl REMPI-TOF spectra. Gas samples from a lecture bottle (Isotec, DCl: 99%) were pumped through a 200 μm pulsed nozzle from a typical backing pressure of about 2 bar into the ionization chamber, which was held at lower than about 10^{-5} mbar pressure during experiments. The distance between the nozzle and the center between the repeller and the extractor was about 4.5 cm. The nozzle was held open for about 80 μs and the laser beam was typically fired about 600 μs after opening of the nozzle. Ions were extracted into a 70 cm long time-of-flight tube and focused with an electric lense onto a MCP plate detector. Voltage outputs as a function of flight time were fed into a LeCroy 9310A, 400 MHz storage oscilloscope. Average voltage outputs for a fixed number of laser pulses were evaluated and recorded on a computer to get mass spectra. Mass peaks of chosen ions were integrated and averaged for a fixed number of laser pulses as a function of laser radiation wavenumbers to obtain REMPI-TOF spectra. Typically spectral points were obtained by averaging over 50 pulses.

Care was taken to prevent power broadening due to ac Stark effects by minimizing laser power. Wavelength calibration was achieved by recording halogen atomic lines [24] or by comparison of the strongest hydrogen chloride rotational lines with those reported by Green et al. [25] The accuracy of the calibration was found to be about ±2 cm^{-1} on the two- and three-photon wavenumber scales. Spectra intensities were corrected for possible intensity drift during the scan. Furthermore, the effect of varying laser power was corrected for by dividing the measured intensity by the power cubed for (3 + 1)REMPI spectra and by the power squared for (2 + 1)REMPI spectra.

3. Spectral analysis

Identification and assignments of excited electronic states was based on the rotational structure of vibrational bands in terms of *positions* and *intensities* of rotational lines. Rotational and vibrational parameters were derived from simulation analysis of the spectra, based on least square analysis of line positions. Deviations from regular patterns in terms of line positions and/or line intensities indicated perturbation effects due to state interactions. Strength of state interactions was evaluated from line displacements.

Rotational line *positions* $(\tilde{\nu}_{J',v'\leftarrow J'',v''}(i))$ for an isotopomer i ($i = 1$ and 2, refer to ^{1}HCl and ^{2}HCl (i.e., DCl), respectively) are derived from the expression

$$\tilde{\nu}_{J',v'\leftarrow J'',v''}(i) = \tilde{\nu}^0_{v'\leftarrow v''}(i) + \Delta E_{J',J''}(i), \quad (1)$$

where $(\tilde{\nu}^0_{v'\leftarrow v''}(i))$ is the band origin of a vibrational band. $\Delta E_{J',J''}(i)$ is the difference in rotational energies in the ground and the excited states [1,7]. The band origin of an isotopomer i can be expressed as a function of the electronic term value of the excited state, T'_e and the vibrational frequencies (in cm^{-1}) of the two states involved ($\omega'_e(i)$ and $\omega''_e(i)$) [4,9,11]. The difference in the rotational energies for isotopomer i ($\Delta E_{J',J''}(i)\,cm^{-1}$) can be expressed as a function of the rotational parameters of the two rovibrational states, $B_{v'}(i)$, $D_{v'}(i)$, $B_{v''}(i)$, and $D_{v''}(i)$. For given rotational parameters for the ground state, simulation of a rovibrational spectrum allows evaluation of the corresponding excited state values as well as the band origin. The vibrational frequencies of the excited states can be evaluated from the isotope shift (i.e., difference in band origins; $\Delta\tilde{\nu}^0 = \tilde{\nu}^0_{v'\leftarrow v''}(i) - \tilde{\nu}^0_{v'\leftarrow v''}(j)$) and the ground state vibrational frequency values

$$\omega'_e(i) = \frac{2\Delta\tilde{\nu}^0}{(1-\rho)} + \omega''_e(i) \quad (2)$$

and

$$\omega_e(j) = \omega_e(i)\rho, \quad \rho = [\mu(i)/\mu(j)]^{1/2}. \quad (3)$$

The simulation procedure assumes centrifugal distortion of a rigid rotor approximation to hold, hence the energy spacing between neighbouring rotational levels ($\Delta E_{J,J-1} = E_J - E_{J-1}$) to be expressed as

$$\Delta E_{J,J-1} = 2BJ - 4DJ^3. \quad (4)$$

Experimental energies of rovibrational levels in the excited states and corresponding spacing values can be evaluated from those in the ground state ($E_{v'',J''}$; $v'' = 0$) and from measured wavenumbers for the corresponding transition ($\tilde{\nu}_{v',J'\leftarrow v'',J''}$)

$$E_{v',J'} = \tilde{\nu}_{v',J'\leftarrow v'',J''} + E_{v'',J''}. \quad (5)$$

Deviations from regular energy level patterns in excited states are believed to be due to state interactions. Level to level interactions are represented by

$$E = (1/2)(E^0_1 + E^0_2) \pm (1/2)\left[4|W_{12}|^2 + (E^0_1 - E^0_2)^2\right]^{1/2}, \quad (6)$$

where E^0_1 and E^0_2 are the zero-order rovibrational level energies for states 1 and 2 and W_{12} is the matrix element of the perturbation function/the interaction strength. The E's are the resulting level energies. Comparison of experimentally observed energy levels (Eq. (5)) and predicted energies, thus allows the interaction strength (W_{12}) to be evaluated from Eq. (6).

Relative line *intensities* (I_{rel}) of spectra recorded at thermal equilibrium are evaluated from

$$I_{rel} = CS_{\Delta\Omega}\exp(-E(J'')hc/k_BT), \quad (7)$$

where $S_{\Delta\Omega}$ is the multi-photon absorption strength. $E(J'')$ is the rotational energy in the ground state (in cm^{-1}). h, c, k_B, and T have the usual meaning and C is an arbitrary constant. The multi-photon absorption strength, $S_{\Delta\Omega}$, is expressed as

$$S_{\Delta\Omega} = s_i\mu_i^2 + s_j\mu_j^2, \quad (8)$$

where s_i and s_j are Hönl-London type [21] functions of the ground and the excited states' total angular momentum quantum numbers (J'' and J') and of the total electronic angular momentum projection quantum numbers (Ω'' and Ω') [1]. μ_i^2 and μ_j^2 are sum and product functions of all one-photon transition moments and energy denominators that give rise to parallel or perpendicular transitions [2,26]. The subscript numbers i and j refer to the order of Clebsch–Gordan coefficients, in terms of which s_i and s_j can be written [26–28]. For two-photon absorption strengths $i = 0$ and $j = 2$ but for three-photon absorption strengths $i = 1$ and $j = 3$. μ_i^2 and μ_j^2 are treated as variables in simulation. Deviations from a regular behavior of line intensities as a function of J quantum numbers as predicted by Eq. (7) indicate state interactions.

4. Results and analysis

The excitation wavenumber range for single color (3 + 1)REMPI of HCl and DCl corresponds to the photon energies between one-fourth and one-third of the ionization potential (IP is 12.748 eV = 102820 cm^{-1}), while the range for (2 + 1)REMPI corresponds to the photon energies between one-third and one-half of it ($(3+1)\text{REMPI}: 25705 < \tilde{\nu}_{LASER}\ cm^{-1} < 34273$ and $(2+1)\text{REMPI}: 34273 < \tilde{\nu}_{LASER}\ cm^{-1} < 51410$). Hence, a common resonance excitation energy range for (n + 1)REMPI (n = 2,3) ($\tilde{\nu}_{exc} = n\tilde{\nu}_{LASER};\ n = 2,3$) is $77115 < \tilde{\nu}_{exc}\ cm^{-1} < 102820$.

Figs. 1A and 2 show the (3 + 1) and (2 + 1)REMPI spectra of HCl, respectively, in the excitation wavenumber range 89000–89600 cm^{-1}. Fig. 3A shows the (3 + 1)REMPI spectrum of DCl in the region 89070–89430 cm^{-1}.

Spectra due to the two-photon resonance transitions $j^3\Sigma^-(0^+) \leftarrow X(^1\Sigma^+)$ ($v' = 0$, $v'' = 0$), $j^3\Sigma^-(1) \leftarrow X(^1\Sigma^+)$ ($v' = 0$, $v'' = 0$) and $V^1\Sigma^-(0^+) \leftarrow X(^1\Sigma^+)$ ($v' = 21$, $v'' = 0$) were identified in the (2 + 1)REMPI spectrum of HCl [29–31]. Three overlapping vibrational bands, two of which are centered at 89168.5 and 89282.0 cm^{-1} are found in this region in the (3 + 1)REMPI spectrum. The complex structure near 89030 cm^{-1} is believed to be due to the $j^3\Sigma^-(1) \leftarrow X(^1\Sigma^+)$ transition and the band centered at 89282 cm^{-1} was identified as the $j^3\Sigma^-(0^+) \leftarrow X(^1\Sigma^+)$ system. The separated experimental spectra of the 89168.5 and 89282.0 cm^{-1} bands (Figs. 1B and C and 4(top)) were formed by plotting peaks

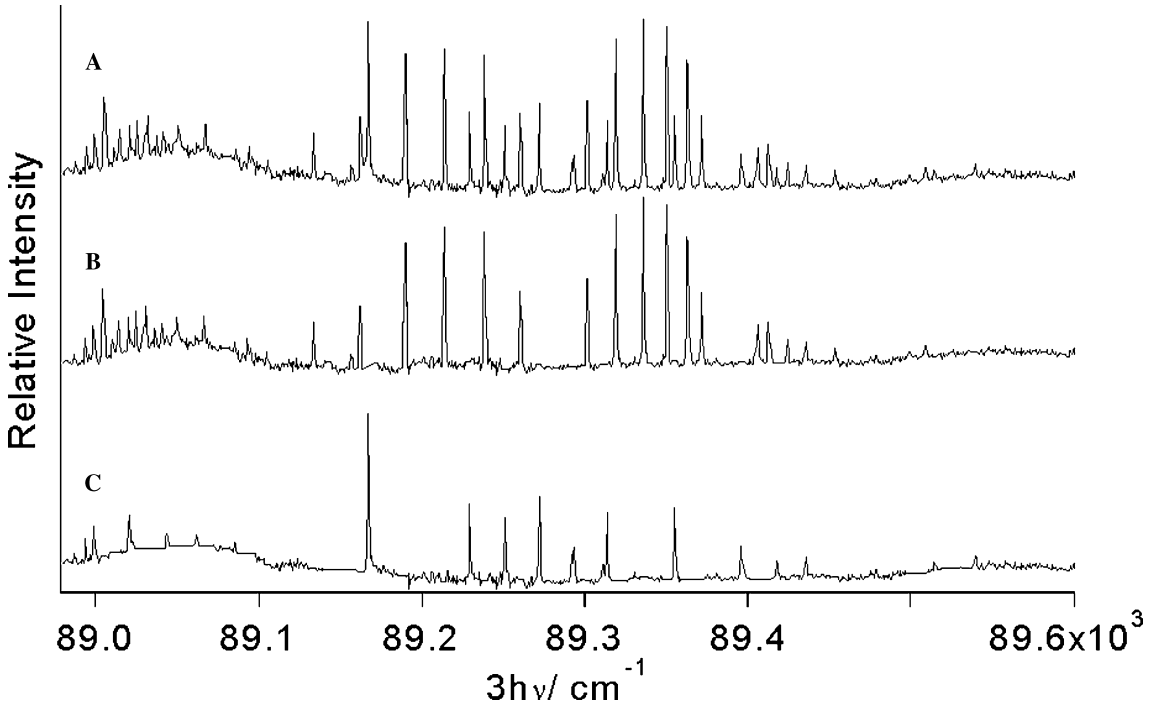

Fig. 1. Experimental (3 + 1)REMPI–current spectrum of HCl (A) due to the three-photon transitions $j(^3\Sigma^-)(0^+) \leftarrow X(^1\Sigma^+)$, ($v' = 0$, $v'' = 0$) (B) and $l(^3\Phi_3) \leftarrow X(^1\Sigma^+)$, ($v' = 0$, $v'' = 0$) (C). Separation of spectral bands (B and C) is based on the analysis mentioned in the text and partly shown in Fig. 4.

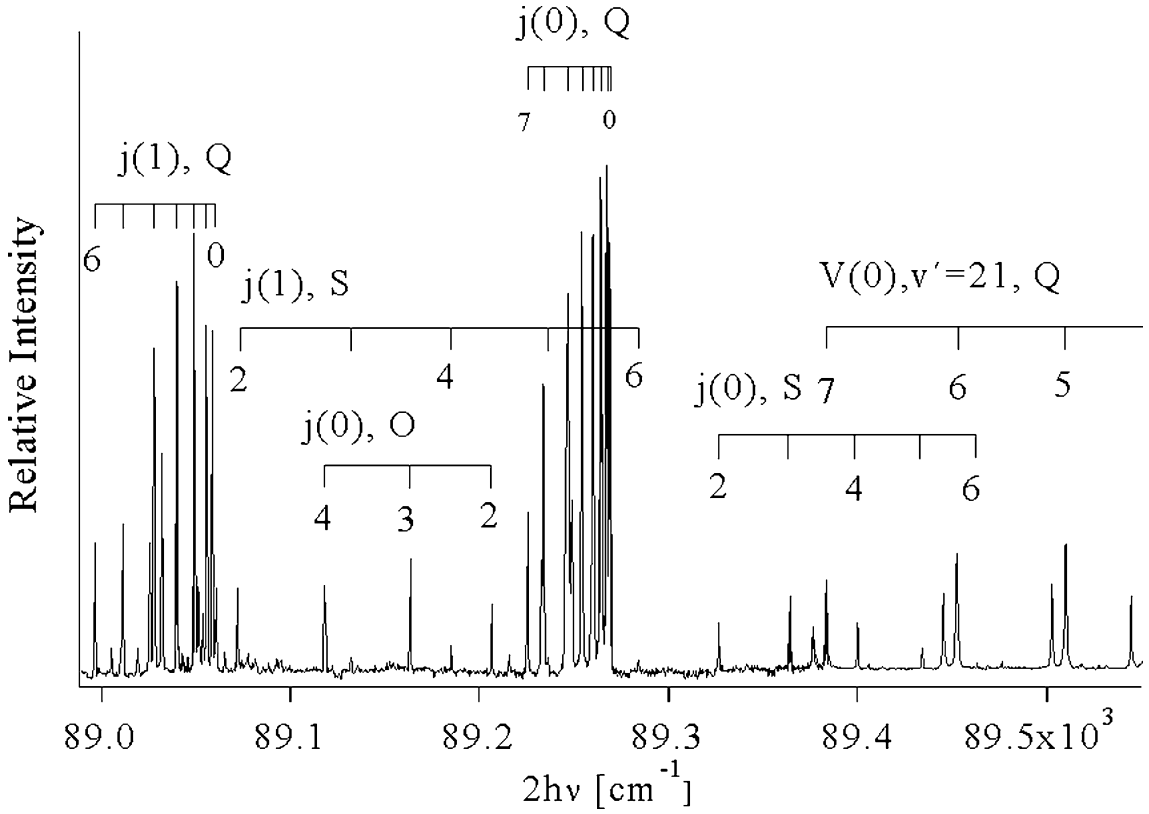

Fig. 2. Experimental (2 + 1)REMPI–current spectrum of HCl, showing spectra due to two-photon transitions (A) $j(^3\Sigma^-)(0^+) \leftarrow X(^1\Sigma^+)$, ($v' = 0$, $v'' = 0$), O, Q, and S line series. (B) $j(^3\Sigma^-)(1) \leftarrow X(^1\Sigma^+)$, ($v' = 0$, $v'' = 0$), Q series. (C) $V(^1\Sigma^+) \leftarrow X(^1\Sigma^+)$, ($v' = 21$, $v'' = 0$), Q series.

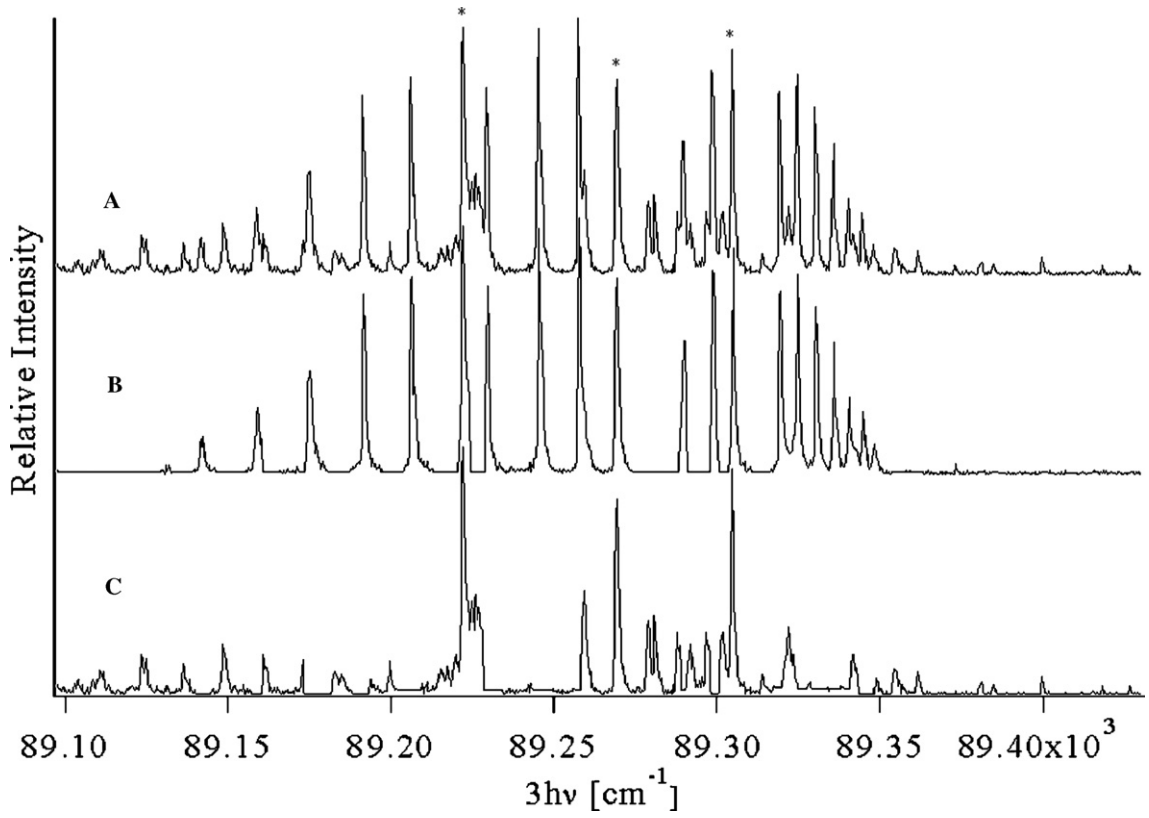

Fig. 3. Experimental (3 + 1)REMPI–TOF spectrum of DCl (A) due to the three-photon transitions $j(^3\Sigma^-)(0^+) \leftarrow X(^1\Sigma^+)$, ($v' = 0$, $v'' = 0$) (B), and $l(^3\Phi_3) \leftarrow X(^1\Sigma^+)$, ($v' = 0$, $v'' = 0$) (C). Separation of spectral bands (B and C) is based on the analysis mentioned in the text. Line overlap is observed for peaks marked with asterisks.

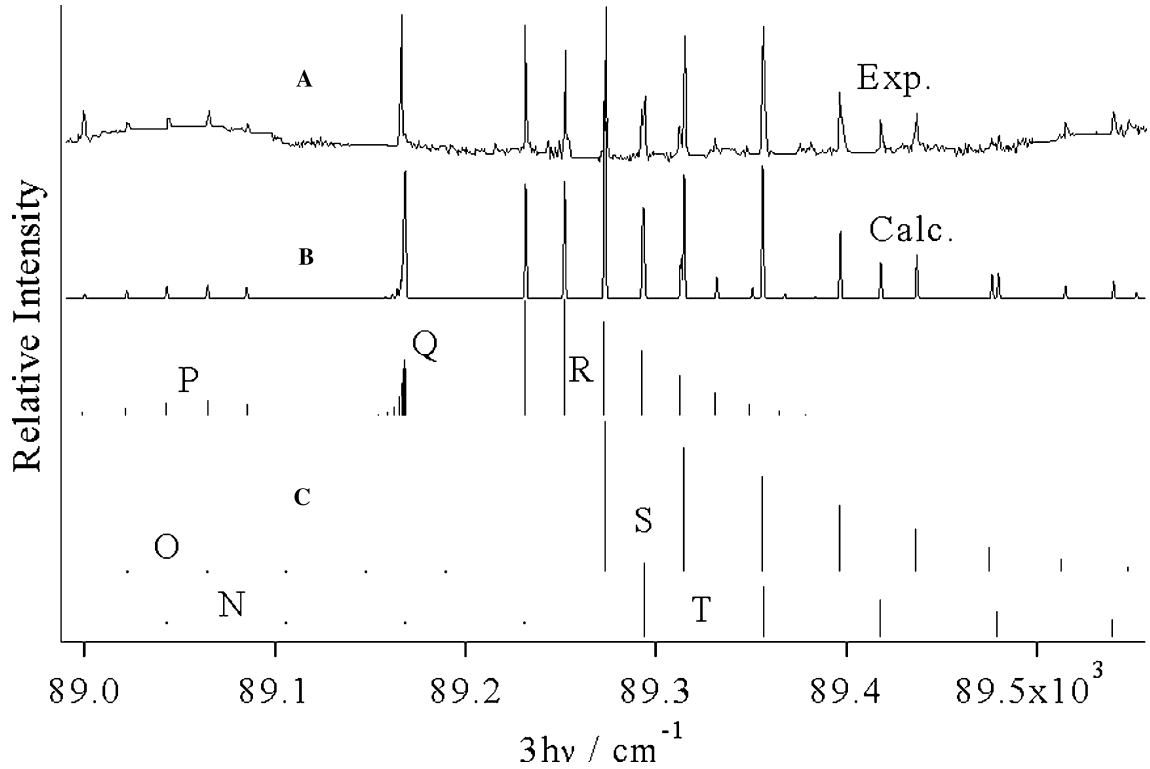

Fig. 4. HCl, $l(^3\Phi_3) \leftarrow X(^1\Sigma^+)$, ($v' = 0$, $v'' = 0$) (3 + 1)REMPI spectrum simulation. Experimental spectrum (A), calculated rotational line contributions (C), and simulated spectrum (B). Rotational line series, N–T, are indicated.

which belong to one of the two bands only, eliminating those belonging to the other band. Straight lines have replaced spectral regions where peaks have been eliminated.

Two overlapping vibrational bands, one at 89228.2 cm^{-1} and another one at 89281.0 cm^{-1} are found in the (3 + 1)REMPI spectrum of DCl. The band at 89281.0 cm^{-1} was identified as the $j^3\Sigma^-(0^+) \leftarrow X(^1\Sigma^+)$ system. The separated experimental spectra are shown in Figs. 3B and C. Furthermore, the Q branch lines of the $j^3\Sigma^-(0^+) \leftarrow X(^1\Sigma^+)$ system were identified in a (2 + 1)REMPI spectrum for DCl.

Noticeably, no transition to the $V^1\Sigma^-(0^+)$ state was observed in the (3 + 1)REMPI spectra, neither for HCl or DCl.

Table 1
Rotational lines of the $l(^3\Phi_3 \leftarrow X(^1\Sigma^+)$, (0,0) band system for (A) HCl and (B) DCl derived from (3 + 1)REMPI spectra (cm^{-1})

J (=J'')	P	Q	R	S	T
(A) HCl					
0					89292.9
1				89272.5	89355.3
2			89230.5	89313.9	89417.1
3		89168.7	89251.5	89355.3	89478.5
4	89085.6		89272.5	89395.5	89539.5
5	89065.1		89291.7	89435.7	
6	89044.2		89311.3		
7	89022.0		89330.1		
8	88999.5				
9					
(B) DCl					
0					89291.4
1				89280.6	89322.9
2			89259.0	89301.7	89354.2
3		89227.6	89269.2	89321.8	89384.
4	89184.4		89278.5	89341.3	
5	89172.7		89287.6	89361.2	
6	89161.1		89296.5	89380.8	
7	89148.3		89304.3		
8	89136.1		89313.6		
9	89123.1				

5. HCl, DCl: $l(^3\Phi_3) \leftarrow X(^1\Sigma^+)$

The spectrum centered at 89168.5 cm^{-1} for HCl (see Fig. 1C) shows the intensity patterns for rotational line series to be expected for an $\Omega' = 3 \leftarrow \Omega'' = 0$ three-photon transition [1,2,4]. Rotational lines are listed in Table 1A. Simulation analyses, shown in Fig. 4, revealed the spectroscopic parameters, $\tilde{\nu}^0$, B', and D' listed in Table 2. This $\Omega = 3$ state has not been observed before. We assign it to the $l(^3\Phi_3)$ state ($v' = 0$) which belongs to the dδ manifold ($(\sigma^2\pi^3)3\,d\delta$) and Rydberg series converging to the higher energy $^2\Pi_{3/2}$ spin–orbit component of the ground ionic state ($X(^2\Pi_\Omega)$), for the following reasons: (1) First, one of four Rydberg states belonging to the dδ manifold and converging to the $^2\Pi_{3/2}$ spin–orbit component of the ground ionic state has been reported in this spectral area, i.e., the $k(^3\Pi_1)(\tilde{\nu}^0 = 88121.6\,cm^{-1})$ state [31]. The remaining states that belong to this category and which are expected to be found in this region are the $k(^3\Pi_0)$, $l(^3\Phi_3)$, and the $l(^3\Phi_4)$ states. (2) Second, the $\Omega' = 3$, singlet state ($L(^1\Phi_3)$), which also belongs to the dδ manifold but converges to the $^2\Pi_{1/2}$ spin–orbit component of the ionic state has been observed at $\tilde{\nu}_0 = 89981.6\,cm^{-1}$, i.e., 813 cm^{-1} higher in energy [4]. This separation is of the same order of magnitude as that of the spin–orbit splitting for the ground state ion (648 cm^{-1}) [32]. (3) Third, the similarity in rotational parameters observed for this state and the ground state ($B' = 10.44\,cm^{-1}$ and $B'' = 10\,439\,826\,cm^{-1}$), implying comparable average internuclear distances for the two potential curves, suggests that the (0,0) band is the dominant vibrational band. Transitions to triplet states in single- and two-photon absorption are generally found to be important in the hydrogen halides, suggesting that spin–orbit coupling is significant in these molecules.

By analogy with the analysis described above for HCl, the band for DCl, centered at 89228.2 cm^{-1} was assigned to the $l(^3\Phi_3)$ state ($v' = 0$). Rotational lines are listed in Table 1B and resulting spectroscopic parame-

Table 2
Band origins (ν^0) vibrational frequencies (ω_e) and rotational parameters (B and D) for HCl and DCl states (vibrational quantum numbers $v = 0$) (cm^{-1})

State	$X^1\Sigma^+$		$l^3\Phi_3$		$j^3\Sigma^-(0^+)$	
Configuration	$\sigma^2\pi^4$		$\sigma^2\pi^3 3d\delta$		$\sigma^2\pi^3 e\sigma$	
Ion core	—		$^2\Pi_{3/2}$		$^2\Pi_{3/2}$	
Compound	HCl	DCl	HCl	DCl	HCl	DCl
ν^0 ours'			89168.5	89228.2	89282.0	89281.0
ν^0 others'					89282.2[b]	
ω_e ours'			2568.7	1842.3	2998.0	2150.2
ω_e others'	2990.9463[a]	2145.163[a]				
B (cm^{-1}) ours'			10.44	5.25	9.64	5.06
B (cm^{-1}) others'	10.439826[a]	5.39215[a]			9.657[b]	
$D \times 10^3$ (cm^{-1}) ours'			1.45	3.57		
$D \times 10^3$ (cm^{-1}) others'	0.50877123[a]	0.13627777[a]			0.871[b]	

[a] See [32].
[b] See [29].

ters, $\tilde{\nu}^0$, B', and D' derived from simulation analyses are listed in Table 2. Furthermore, vibrational frequencies (in wavenumbers) of the excited states for both compounds ($\omega'_e(1)$ and $\omega'_e(2)$) could be estimated from the isotope shift value ($|\Delta\tilde{\nu}^0| = 59.7\,\mathrm{cm}^{-1}$; Eqs. (2) and (3)).

6. HCl, DCl: $j(^3\Sigma^-(0^+)) \leftarrow X(^1\Sigma^+)$

Spectra due to the transition $j(^3\Sigma^-(0^+)) \leftarrow X(^1\Sigma^+)$ are identified both in (2 + 1) and (3 + 1)REMPI. O, Q, and S line series are observed in the (2 + 1)REMPI spectrum, while mainly P, R, and to a lesser extent N and T lines, are observed in (3 + 1)REMPI as to be expected for $\Delta\Omega = 0$ ($\Omega' = 0 \leftarrow \Omega'' = 0$) transitions [2]. Irregularity in line positions and line intensities is clearly observed in the Q ((2 + 1)REMPI) and R ((3 + 1)REMPI) line series for HCl and DCl as well as in the P ((3 + 1)REMPI) line series for DCl. Correlation between line positions and transitions to upper state rovibrational levels, which gives consistent energy level position (Eq. (5)) is shown in Fig. 5 for HCl and in Fig. 6 for DCl. Averaged rotational level energies are listed in Table 3. Spacing between levels ($\Delta E_{J',\,J'-1}$), derived from corresponding spectra, is also plotted in Fig. 5. Clearly deviations from a regular pattern for $\Delta E_{J',\,J'-1}$ as a function of energy (or J; see Eq. (4)) are seen both for HCl and DCl. This shows most clearly as enhanced spacing between levels $J' = 7$ and 8 in HCl and between levels $J' = 3$ and 4 in DCl. Rotational line intensities vs J' for HCl are plotted in Fig. 7. This shows consistent drops in line intensities to minimum values for those lines corresponding to transitions to $J' = 7$. These observations are consistent with near resonant state interactions between the $j(^3\Sigma^-(0^+))$ and the $V(^1\Sigma^+)$ states.

Deperturbed quantum levels of the $V(^1\Sigma^+)$, $v' = 24$ state evaluated by Liyanage et al. are close in energy to those of the $j(^3\Sigma^-(0^+))$, $v' = 0$ state for HCl as shown in Fig. 5. More precisely, the energies of the $J' = 7$ ($E_{v'=24,\,J'=7} = 91\,337\,\mathrm{cm}^{-1}$) and 8 ($E_{v'=24,\,J'=8} = 91\,403\,\mathrm{cm}^{-1}$) quantum levels of the V state are in the energy range marked by the levels with the same quantum numbers of the j state ($E_{0,7} = 91\,307\,\mathrm{cm}^{-1}$; $E_{0,8} = 91\,481\,\mathrm{cm}^{-1}$). The enhanced energy-gap observed between these levels in the $j(^3\Sigma^-(0^+))$ state (Fig. 5), therefore can be explained as being due to a level-to-level repulsion between the $j(^3\Sigma^-(0^+))$ and the $V(^1\Sigma^+)$ states with same J quantum numbers [6,7]. The drop in line intensities for levels close to $J' = 7$ in $j(^3\Sigma^-(0^+)) \leftarrow X(^1\Sigma^+)$ (Fig. 7) suggests an enhanced mixing with the V state. Judging from the fact that no three-photon absorption due to the $V \leftarrow X$ transition is observed, an enhanced mixing with the V state will cause a decrease in transition probabilities, hence giving rise to a lowering in intensities.

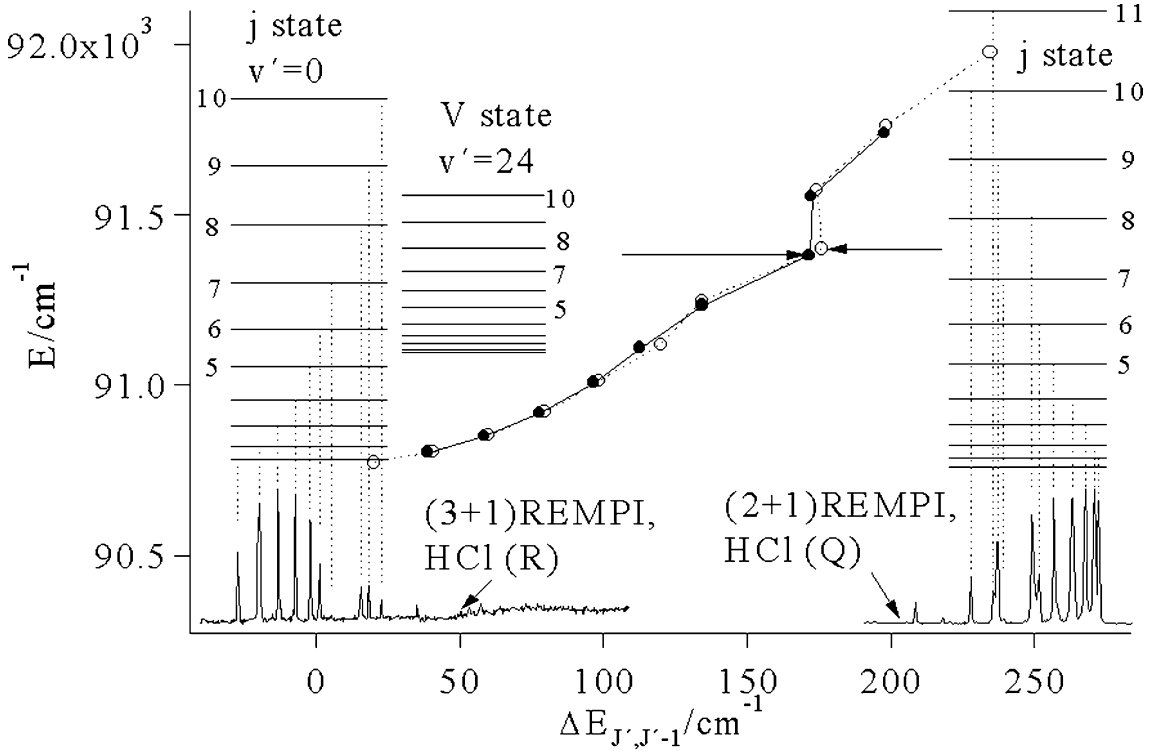

Fig. 5. REMPI spectra of HCl; correlation between rotational line positions and transitions to upper state rovibrational levels in the $j(^3\Sigma^-)(0^+)$ state, for P lines in (3 + 1)REMPI to left and for Q lines in (2 + 1)REMPI to right. Spacings between rotational lines ($\Delta E_{J',\,J'-1}$) are plotted as $\Delta E_{J',\,J'-1}$values along the x axis vs energies (E) along the y axis in the middle of the figure (filled circles from the R line spectrum; open circles from the Q line spectrum). Rotational levels for the $V(^1\Sigma^+)$, $v' = 24$ state are also shown. J' numbers are indicated.

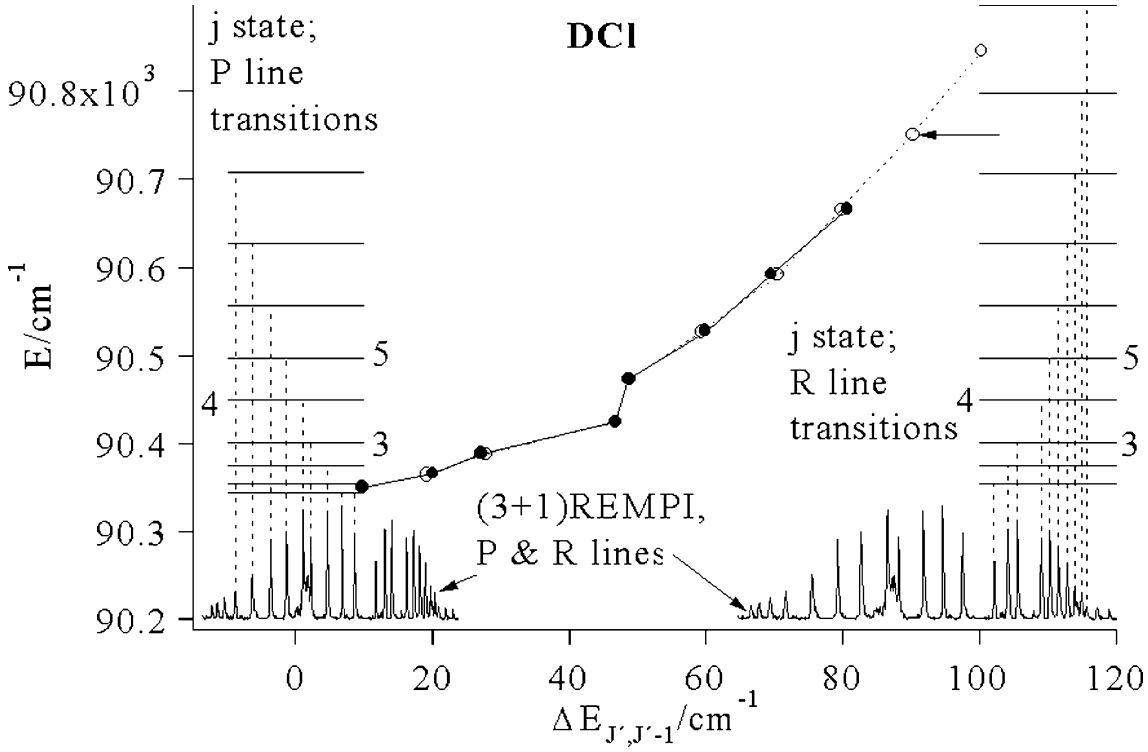

Fig. 6. (3 + 1)REMPI spectra of DCl; correlation between rotational line positions and transitions to upper state rovibrational levels in the $j(^3\Sigma^-)(0^+)$ state, for P lines to left and for R lines to right. Spacings between rotational lines ($\Delta E_{J',J'-1}$) are plotted as $\Delta E_{J',J'-1}$ values along the x axis vs energies (E) along the y axis in the middle of the figure (filled circles from the P line spectrum; open circles from the R line spectrum). J' numbers are indicated.

Table 3
Rotational energy levels of the $j(^3\Sigma^-)(0^+)$, $v' = 0$ states for HCl and DCl derived from analysis of (3 + 1) and (2 + 1)REMPI spectra (see Figs. 5 and 6) (cm^{-1})

J'	HCl	DCl
0	90764	90346
1	90784	90356
2	90823	90375
3	90882	90403
4	90960	90449
5	91057	90498
6	91173	90558
7	91307	90628
8	91481	90708
9	91654	90798
10	91852	90898
11	92096	

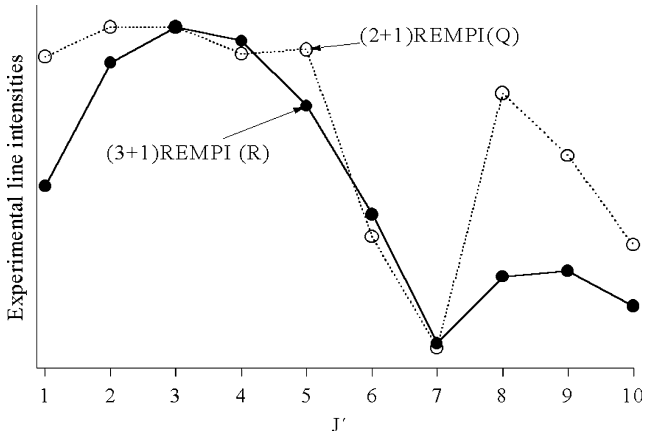

Fig. 7. HCl. Relative experimental line intensities as functions of J' quantum numbers for (A) R lines in the (3 + 1)REMPI spectrum (filled circles) and (B) Q lines in the (2 + 1)REMPI spectrum (open circles) for the transitions from $X(^1\Sigma^+)$, $v'' = 0$ to $j(^3\Sigma^-)(0^+)$, $v' = 0$.

Perturbation analyses of the energy level pattern (Fig. 5) for the j state, based on level-to-level interactions (Eq. (6)), revealed interaction strength (W_{12}) between $j(^3\Sigma^-(0^+))$, $v' = 0$ and $V(^1\Sigma^+)$, $v' = 24$ of the order $20 \pm 4\,cm^{-1}$.

Similarly, for DCl, deperturbed quantum levels of the $V(^1\Sigma^+)$, $v' = 33$ state are found to be close in energy to those of the $j(^3\Sigma^-(0^+))$, $v' = 0$ state [19]. Hence, the enhanced energy-gap observed between levels $J' = 3$ and 4 in the $j(^3\Sigma^-(0^+))$ state (Fig. 6) we believe is also due to a level-to-level repulsion interaction between the two states. Furthermore, analogous, although not quite as clear, line intensity alterations were seen in the DCl spectra as in the HCl spectra (see above). Perturbation analysis of the energy level pattern (Fig. 6) for the j state revealed interaction strength between $j(^3\Sigma^-(0^+))$, $v' = 0$ and $V(^1\Sigma^+)$, $v' = 33$ of the order $7 \pm 2\,cm^{-1}$.

To a first approximation the interaction strength is proportional to the square of the overlap integral of the vibrational wavefunctions of concern. A wavefunction

with higher vibrational quantum number for the interacting V state in DCl ($v' = 33$) compared to the vibrational quantum number of the wavefunction in HCl ($v' = 24$) will indeed overlap to a lesser extent with the corresponding $v' = 0$ wavefunctions in the j state to give rise to lower interaction strength as observed ($7 \pm 2\,\mathrm{cm}^{-1}$ for DCl vs $20 \pm 4\,\mathrm{cm}^{-1}$ for HCl).

7. Conclusions

(3 + 1) and (2 + 1)REMPI spectra for total current detection (HCl) and molecular ion detection (DCl) over the spectral region 89 000–89 600 cm^{-1} were recorded.

Simulation calculations based on Hönl-London-type expressions for rotational line strengths in three-photon absorptions allowed identification and characterization of new $\Omega' = 3$ states in HCl and DCl in (3 + 1)REMPI spectra. The states are assigned as the $I(^3\Phi_3)$ Rydberg states for vibrational quantum numbers $v' = 0$ and electronic configurations $(\sigma^2\pi^3)3d\delta$ which belong to series converging to the $\Omega = 3/2$ spin–orbit component of the ground state molecular ions ($X(^2\Pi_\Omega)$). The analyses allowed evaluation of band origins and rotational constants for the excited states.

Spectra due to the transition $j(^3\Sigma^-(0^+)) \leftarrow X(^1\Sigma^+)$ were identified in the spectral region investigated. Consistent irregularities in rotational line positions as well as line intensities were observed in the various line series both in (2 + 1) and (3 + 1)REMPI spectra. These could be interpreted as being due to near resonance homogeneous state interactions with the ion-pair states $V(^1\Sigma^+)$, $v' = 24$ for HCl and $v' = 33$ for DCl. Interaction strengths were evaluated from perturbation analysis of the data.

Acknowledgments

The financial support of the University Research Fund, University of Iceland, and the Icelandic Science Foundation is gratefully acknowledged. We also thank Jón Matthíasson and Oddur Ingólfsson for useful help with the project.

References

[1] Á. Kvaran, B.G. Waage, H. Wang, J. Chem. Phys. 113 (2000) 1755–1761.
[2] Á. Kvaran, H. Wang, B.G. Waage, Can. J. Phys. 79 (2001) 197–210.
[3] H. Wang, Á. Kvaran, J. Mol. Struct. 563-564 (2001) 235–239.
[4] Á. Kvaran, H. Wang, Mol. Phys. 100 (2002) 3513–3519.
[5] D. Ascenzi, S. Langford, M. Ashfold, A. Orr-Ewing, Phys. Chem. Chem. Phys. 3 (2001) 29–43.
[6] Á. Kvaran, H. Wang, Á. Logadóttir, J. Chem. Phys. 112 (2000) 10811–10820.
[7] Á. Kvaran, Á. Logadóttir, H. Wang, J. Chem. Phys. 109 (1998) 5856–5867.
[8] Á. Kvaran, H. Wang, Á. Logadóttir, in: Recent Research Development in Physical Chemistry, vol. 2, Transworld Research Network, 1998, pp. 233–244.
[9] G.H. Jóhannesson, H. Wang, Á. Kvaran, J. Mol. Spectrosc. 179 (1996) 334–341.
[10] Á. Kvaran, G.H. Jóhannesson, H. Wang, Chem. Phys. 204 (1996) 65–75.
[11] Á. Kvaran, H. Wang, G.H. Jóhannesson, J. Phys. Chem. 99 (1995) 4451–4457.
[12] D.S. Green, G.A. Bickel, S.C. Wallace, J. Mol. Spectrosc. 150 (1991) 354–387.
[13] D.S. Green, S.C. Wallace, J. Chem. Phys. 96 (1992) 5857–5877.
[14] Y. Xie, P.T.A. Reilly, S. Chilukuri, R.J. Gordon, J. Chem. Phys. 95 (1991) 854–864.
[15] R. Callaghan, R.J. Gordon, J. Chem. Phys. 93 (1990) 4624–4636.
[16] S.G. Tilford, M.L. Ginter, J. Mol. Spectrosc. 40 (1971) 568–579.
[17] R.F. Barrow, J.G. Stamper, Proc. R. Soc. A 263 (1961) 259–276.
[18] R.F. Barrow, J.G. Stamper, Proc. R. Soc. A 263 (1961) 277–288.
[19] R. Liyanage, R.J. Gordon, R.W. Field, J. Chem. Phys. 109 (1998) 8374–8387.
[20] R.J. Donovan, A.C. Flexen, K.P. Lawley, T. Ridley, Chem. Phys. 226 (1998) 217–228.
[21] G. Herzberg, Molecular Spectra and Molecular Structure; I. Spectra of Diatomic Molecules, second ed., Van Nostrand Reinhold, New York, 1950.
[22] W. Huasheng, J. Ásgeirsson, Á. Kvaran, R.J. Donovan, R.V. Flood, K.P. Lawley, T. Ridley, A.J. Yencha, J. Mol. Struct. 293 (1993) 217–222.
[23] Á. Kvaran, H. Wang, J. Ásgeirsson, J. Mol. Spectrosc. 163 (1994) 541–558.
[24] R.J. Donovan, R.V. Flood, K.P. Lawley, A.J. Yencha, T. Ridley, Chem. Phys. 164 (1992) 439–450.
[25] D.S. Green, G.A. Bickel, S.C. Wallace, J. Mol. Spectrosc. 150 (1991) 388–469.
[26] J.B. Halpern, H. Zacharias, R. Wallenstein, J. Mol. Spectrosc. 79 (1980) 1–30.
[27] E.U. Condon, G.H. Shortley, The Theory of Atomic Spectra, Cambridge University Press, Cambridge, 1963.
[28] D.L. Falkoff, G.S. Colladay, R.E. Sells, Can. J. Phys. 30 (1952) 253–256.
[29] D.S. Green, G.A. Bickel, S.C. Wallace, J. Mol. Spectrosc. 150 (1991) 303–353.
[30] A.E. Douglas, F.R. Greening, Can. J. Phys. 57 (1979) 1650–1661.
[31] D.S. Ginter, M.L. Ginter, J. Mol. Spectrosc. 90 (1981) 177–196.
[32] K.P. Hüber, G. Herzberg, Constants of Diatomic Molecules, Van Nostrand Reinhold, New York, 1979.